Mat. Res. Soc. Symp. Proc. Vol. 693 © 2002 Materials Research Society

Theory of Electron Energy Loss Spectroscopy and its Application to Threading Edge Dislocations in GaN

C. J. Fall,[1] R. Jones,[1,*] P. R. Briddon,[2] A. T. Blumenau,[3] T. Frauenheim,[3] and M. I. Heggie[4]

[1]*School of Physics, University of Exeter, Exeter EX4 4QL, United Kingdom*
[2]*Department of Physics, University of Newcastle upon Tyne, Newcastle NE1 7RU, United Kingdom*
[3]*Theoretische Physik, Universität Paderborn, D-33098 Paderborn, Germany*
[4]*CPES, University of Sussex, Falmer, Brighton BN1 9QJ, United Kingdom*

ABSTRACT

The electronic structure of dislocations in GaN is controversial. Several experimental techniques such as carrier mobility studies and cathodoluminescence experiments have indicated that dislocations are charged while theoretical studies point to intrinsic states and/or point defect accumulation along the core as a source of electrical activity. Electron Energy Loss Spectroscopy (EELS) studies have the ability to probe the electronic structure of extended defects. Here we report first principles calculations of the EELS spectrum applied to edge dislocations in GaN. It is found that the electrostatic potential at N atoms in the vicinity of the dislocation varies by the order of a volt and casts doubt on any simple interpretation of core loss spectroscopy. On the other hand, low loss spectroscopy leads directly to detailed information about any gap states. The low loss spectrum obtained by the theory is in good agreement with recent experimental work and indicates that threading dislocations in *p*-type GaN possess acceptor levels in the upper half of the gap.

INTRODUCTION

The atomic and electronic structures of dislocations in GaN is a topic of current high interest and is still controversial [1]. Nano-pipes associated with open-core threading screw dislocations have been imaged by transmission electron microscopy (TEM) [2, 3], but full-core structures have also been seen for edge, screw, and mixed dislocations using Z-contrast imaging [4]. The electrical and structural properties of screw dislocations have been found to depend sensitively on the growth conditions [5]. Full-core structures are expected to lead to gap states, which, if filled, would lead to dislocation line charging. Scanning capacitance spectroscopy results have suggested that GaN threading dislocations are negatively charged [6], as have electron holography measurements [7]. A recent ballistic electron emission microscopy study has however concluded that threading dislocations do not have a fixed negative charge, and are, if anything, positively charged at the surface [8].

Initial theoretical investigations of GaN screw and edge dislocations suggested that dislocation core reconstructions lead to a lack of deep gap states [9]. Subsequent calculations, however, have predicted deep levels associated with GaN edge dislocations, leading in particular to charge accumulation at dislocations [10, 11]. Furthermore, a recent theoretical study of GaN edge dislocations has shown evidence for empty gap-states associated with full-core GaN edge dislocations in the top half of the gap [12]. Theoretical work has also shown that Ga-filled screw dislocations—which are also compatible with

experimental observations—are more likely to be formed under Ga-rich conditions than full-core structures [13].

Spatially-resolved electron energy loss (EEL) spectroscopy has the ability to probe the electronic structure of extended defects. When taken on a dislocation core, the EEL spectra can in principle yield valuable information about the electronic structure of the dislocation, both within and above the band gap. Such information could prove crucial to help resolve whether any electrical or optical activity is associated with undecorated dislocations. Energy-loss spectra induced by excitations of N core electrons conveniently allow unoccupied conduction and gap states to be probed. In particular, nitrogen K-edge spectra collected near a pure GaN edge dislocation have shown an increase in absorption just above the band gap compared to bulk regions [4]. Furthermore, core-loss EEL spectra taken near stacking faults in cubic GaN have shown unoccupied gap states 0.6–1.8 eV below the bulk band edge [14]. Low-loss EEL spectroscopy, in the 0–20 eV range, where the energy-loss is induced by exciting electrons from the valence to the conduction bands, is another sensitive technique that can be performed in a scanning TEM that leads directly to detailed information about gap states. Cross-sectional low-loss EEL experiments in GaN have shown differences in the onset of the EEL spectrum on and off threading dislocations [15]. Similar EEL experiments performed near dislocations in Si [16] and diamond [17] have also shown differences between dislocations and bulk regions. In this study, we perform first-principles simulations of a variety of GaN edge dislocation cores, and, by means of a simple model, we determine how dislocations lead to changes in EEL spectra compared with bulk regions.

FIRST-PRINCIPLES METHOD

We perform self-consistent *ab initio* simulations of wurtzite GaN and AlN within the local density approximation (LDA) to density functional theory, using the recently-enhanced AIMPRO code [18]. We use pseudopotentials [19] to describe the ion cores and include the non-linear core correction to account for the Ga 3*d* electrons. Test calculations are also performed with the Ga 3*d*-electrons included as valence electrons. The charge density is expanded in plane waves up to a cutoff of 300 Ry. Wave functions, however, are described using localized *s*, *p*, and *d* atom-centered Gaussian orbitals that are optimized for bulk systems. Structural optimizations are performed with a *dppp* basis on each atom (*i.e.* one *spd* function with a small Gaussian exponent, and three *sp* functions with increasing Gaussian exponents), while EEL spectra are calculated with a Ga (Al) *dddd* basis and a N *dppp* basis. Tests performed with other basis sets have shown only small changes in the atomic and band structures. A grid of Monkhorst-Pack (MP) k-points is used to perform the Brillouin zone (BZ) integrations. The bulk lattice parameters, computed with 24 reduced k-points, are given in Table I. A comparison between our band structures and previous calculations shows only small differences [20, 21]. For example, we obtain valence band widths of 1.13, 2.58, and 7.56 eV with the Ga 3*d* orbitals in the valence states (against band widths of 0.98, 2.65, and 7.26 eV respectively in a previous linear-combination-of-atomic-orbitals calculation [20]). The computed GaN band gap is 1.92 eV, including the Ga 3*d* orbitals, compared with 2.04 eV previously [21]. For AlN, we obtain valence band widths of 3.01 and 6.18 eV (against 2.89 and 6.16 eV previously [20]).

We consider two complementary approaches when describing dislocations: (*a*) a pair of edge dislocations with opposite Burgers vectors is inserted in a 144-atom supercell, or

TABLE I: Theoretical bulk lattice constants (a, c) and bulk modulus (B) for wurtzite GaN and AlN. The stared values indicate results obtained with the Ga $3d$ electrons treated as valence states. Experimental values are indicated in parentheses.

	GaN	AlN
a [a.u.]	5.98 (6.03)[a]	5.79 (5.88)[b]
c/a	1.626 (1.626)[a]	1.62 (1.601)[b]
B [GPa]	208, 216* (237±31)[c]	213 (207.9±6.3)[d]

[a]from Ref. 22.
[b]from Ref. 23.
[c]from Ref. 24.
[d]from Ref. 25.

(b) a single edge dislocation is included in a 120-atom supercell-cluster hybrid, where the surface dangling bonds are saturated by additional fractionally-charged hydrogen-like atoms. Screw dislocations are studied using approach (b) with 108 Ga and N atoms. Both techniques describe [0001] dislocations of infinite length. The periodicity of the structures along in the [0001] direction is fixed at the bulk value of the c-axis. In approach (a), the dislocations are arranged in a quadrupole lattice to minimize strain effects [26]. In approach (b), we include at least 20 a.u. of vacuum around the surface hydrogen atoms. Initial relaxations of the dislocation cores are performed using the self-consistent charge density functional tight-binding method (scc-DFTB) [27], with clusters of up to 500 atoms. The atoms are then further relaxed with AIMPRO to their equilibrium positions, using 2 reduced MP k-points along the [0001] direction.

ENERGY-LOSS SPECTRA THEORY

Low-loss EEL spectra result from electronic transitions between filled valence bands (VB) and empty conduction bands (CB). Transitions involving gap states contribute to the EEL spectra and allow defects to be probed. The signal obtained experimentally is representative of $-\mathrm{Im}\ \varepsilon(E)^{-1}$, where $\varepsilon = \varepsilon_1 + i\varepsilon_2$ is the dielectric function and E is the energy loss [28]. We calculate the diagonal elements of the imaginary part of the dielectric function in the dipole approximation for an applied electron beam oriented along a direction $\hat{\mathbf{e}}_l$ [29, 30]:

$$\varepsilon_2^l(E) = \frac{4\pi e^2}{\Omega} \sum_{c,v} \int d^3\mathbf{k} |\langle \Psi_{\mathbf{k}}^c | \mathbf{r} \cdot \hat{\mathbf{e}}_l | \Psi_{\mathbf{k}}^v \rangle|^2 \delta(E_{\mathbf{k}}^c - E_{\mathbf{k}}^v - E) \quad (1)$$

where Ω is the unit cell volume, and $|\Psi_{\mathbf{k}}^{v,c}\rangle$ are VB and CB states, with energies $E_{\mathbf{k}}^{v,c}$ respectively. The LDA band-gap is adjusted to the experimental value by shifting the conduction bands [31]. Gap states are shifted proportionally to their distance from the valence band. The real part of the dielectric function is obtained through a Kramers-Kronig (KK) transformation. Traditionally, EEL spectra are presented with a Lorentzian broadening scheme, which has the advantage of allowing KK transforms to be computed analytically [32]. However, Lorentzian functions have long tails which tend to mask spectral features at low energy in the band-gap region. Instead, we use here a new

polynomial broadening scheme. The advantage of this broadening function is that is has both a finite width and an analytical KK transform. In Eq. 1, the $\delta(x)$ function is replaced by a normalised polynomial function:

$$f(x) = \begin{cases} \frac{15}{16\beta^5}(x^4 - 2\beta^2 x^2 + \beta^4), & \text{for } -\beta \leq x \leq +\beta \\ 0, & \text{otherwise} \end{cases} \quad (2)$$

which has a full width at half maximum of $\Delta x = 2\beta\sqrt{1 - 2^{-1/2}}$. In the following, we set $\Delta x = 0.8$ eV.

K-edge core-excitation EEL spectra in GaN result from electronic transitions between N $1s$ core electrons and empty gap or conduction band states. Neglecting final-state interactions between the excited electron and the core hole as a first approximation, and in view of the strong localization of the initial state, the core EEL spectra is related to the p-like projected local density of states on the excited N atoms. The measured core-loss EEL intensity $I(E)$ is thus given by:

$$I(E) \approx \sum_{\mathbf{R}} \sum_{c} \int d^3\mathbf{k} |\langle \Psi^c_{\mathbf{k}} | p_{\mathbf{R}} \rangle|^2 \delta(E^c_{\mathbf{k}} - E^i_{\mathbf{R}} - E) \quad (3)$$

where the sum over $\mathbf{R}$ includes all N atoms that contribute to the measured signal, $p_{\mathbf{R}}$ represents a p-like state centered at $\mathbf{R}$, and $E^i_{\mathbf{R}}$ is the energy of the core level at $\mathbf{R}$. In the vicinity of a defect, such as a dislocation, changes in the atomic bonding will induce local potential variations that shift the core-level energies. We therefore decompose $E^i_{\mathbf{R}}$ into $E^i_{\mathbf{R}} = \overline{E} + \Delta E_{\mathbf{R}}$, where $\overline{E}$ is an average value of the core energy level, taken over a suitable volume, and $\Delta E_{\mathbf{R}}$ is the energy difference between this average and the core energy on the N atom of interest. We take the total potential differences—including the Hartree, exchange-correlation, and local pseudopotential terms—to represent the shifts of the N core levels. We display core-level EEL spectra with a Gaussian broadening of 0.8 eV.

The BZ integrations in Eqs. 1 and 3 are performed in bulk material using 1024 MP k-points and a similar k-point density in the supercells. A test calculation for bulk material with 2000 MP k-points yielded very similar results. In this work, EEL spectra are computed assuming p- or n-type material, and hence neutral or negatively-charged full-core edge dislocations respectively [10]. The effect of the Ga $3d$ states on the GaN EEL spectra has been investigated in test calculations by including them fully in the pseudopotential. Only small changes in the resulting EEL spectra were found in the 0–10 eV range.

The influence of dislocations on the EEL spectra is determined by applying Eqs. 1 and 3 to the supercells containing dislocations. In view of the number of atoms in our supercells, we are therefore modeling an EEL spectrum acquired with an electron beam probe diameter of 10–15 Å, centered exactly at the dislocation core. This size is similar to current experimental values [15].

RESULTS AND DISCUSSION

The theoretical low-loss EEL spectra of bulk GaN and AlN are shown in Fig. 1, together with corresponding experimental data, acquired in a cross-sectional geometry with an electron beam in the x, y plane. EEL spectra for x and y orientations are identical because of the 3-fold symmetry of the wurtzite crystal. A good qualitative agreement

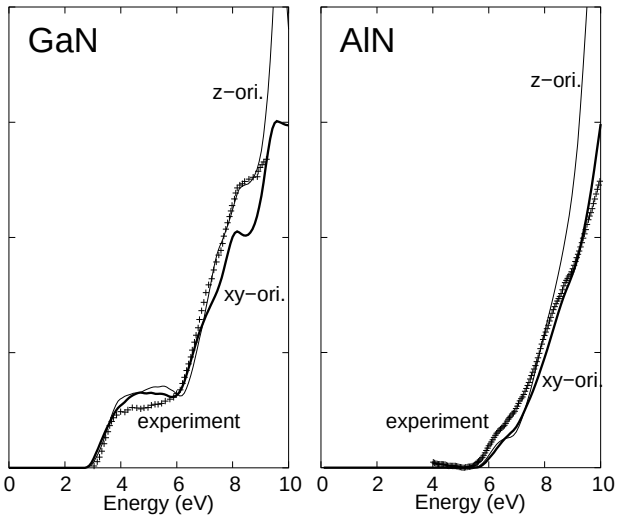

FIG. 1: Comparison between experimental [33] (crosses) and theoretical (lines) low-loss EEL spectra of bulk wurtzite GaN and AlN. The theoretical curves are given for x, y (solid line) and z [0001] (dashed line) orientations of the electron beam and are given in arbitrary units. Experimental spectra are taken with a $[2\bar{1}\bar{1}0]$ incident beam, corresponding to the theoretical x, y curve.

TABLE II: Bond lengths in Å (b_l) and bond angles in degrees (θ) of atoms at neutral GaN edge dislocation cores, computed using the two different approaches described in the text. The atoms labels are shown in Fig. 2 Bulk values are $b_l = 1.94$ Å and $\theta = 109.5°$.

	(a) Supercell approach		(b) Cluster hybrid approach	
Atom	b_l	θ	b_l	θ
A (N)	1.89–1.91	101–105	1.86–1.90	101–102
A (Ga)	1.88–1.89	104–117	1.87–1.88	107–119
B (N)	1.88–1.91	99–113	1.87–1.93	106–113
B (Ga)	1.90–1.91	98–117	1.90–1.94	93–121
D (N)	1.99–2.12	85–133	1.99–2.12	92–129
D (Ga)	1.99–2.11	83–135	1.99–2.10	90–132

between the peaks and shoulders of the x, y computed and measured EEL signals is found. This close correspondence gives us confidence in our approach and parameters, and allows us to extend our study to examine the effect of dislocations on the EEL spectra.

The relaxed geometry of a neutral GaN threading edge dislocation is shown in Fig. 2. The bond lengths and bond angles for the relaxed core atoms are reported in Table II. At the dislocation core, the three-fold coordinated atoms labelled A in Fig. 2a are separated, in the $[10\bar{1}0]$ direction, by 0.21 Å using approach (a) and by 0.31 Å using approach (b). The corresponding electronic band structures are shown in Fig. 2. In both approaches, empty states localized at the core of the dislocation are found in the upper half of the gap. In the supercell calculation with two dislocations per unit cell, shown in Fig. 2a, the two dislocation cores give rise to two sets of gap states, which mix because of the restricted supercell size and are seen to be split at the Brillouin zone center. A test calculation

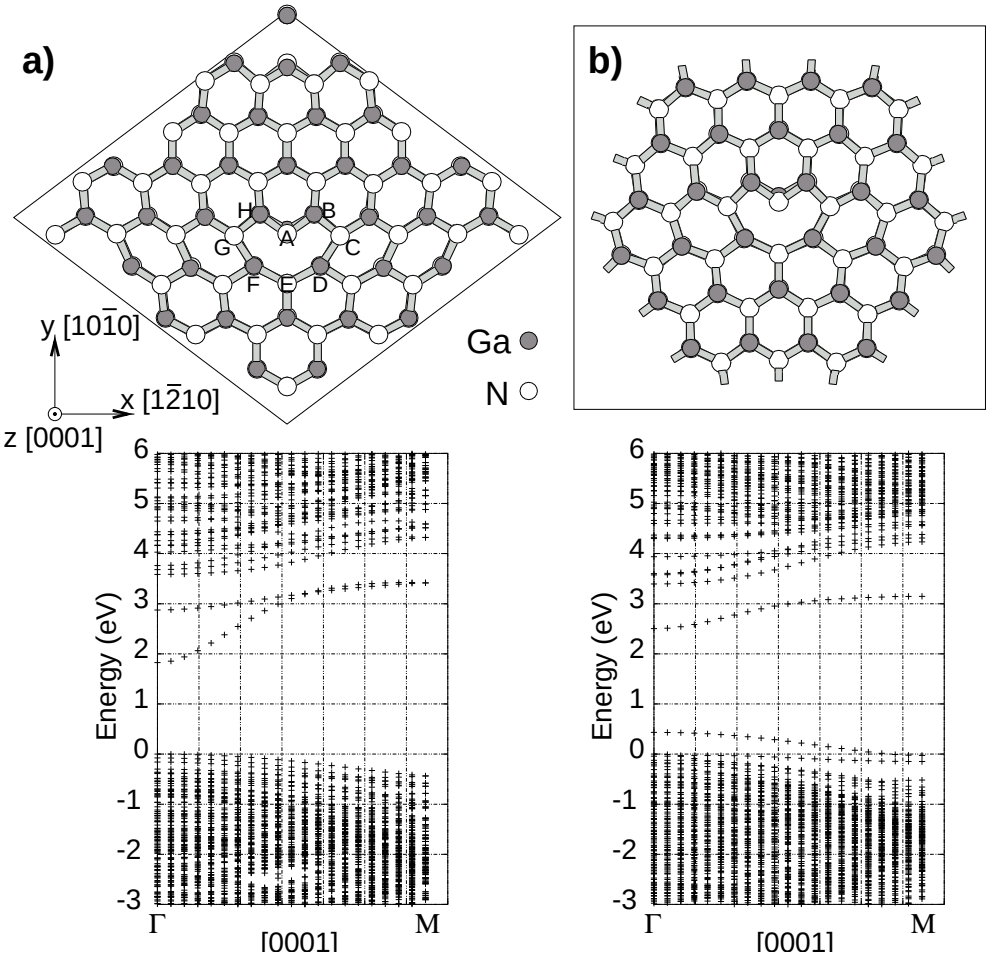

FIG. 2: Upper panels: Two complementary approaches to describe dislocations: a) a GaN supercell containing two edge dislocations; b) a GaN single edge dislocation surrounded by vacuum, where the surface bonds are saturated by fractional hydrogen atoms (not shown). Both structures have been fully relaxed in the neutral charge state. The N atoms are shown in white and Ga atoms in grey. The core atomic columns are indexed with capital letters. Lower panels: Corresponding band structures in the [0001] *c*-direction. The reference energy has been set at the top of the filled valence states. All levels in the top (bottom) half of the gap are empty (filled, respectively).

performed with a larger 312-atom supercell containing a dislocation dipole yielded essentially the same band structure as that of Fig. 2a, with two gap states in the top half of the gap. Both states are centred on the dislocation core, and decay around the dislocation. The central part of the wave functions is formed by Ga-related *sp*-orbitals. The lower-energy wave function principally mixes orbitals related to Ga atoms in the columns labelled A, D, and F in Fig. 2a, while the upper state mixes orbitals related to Ga atoms in columns A, E, B, and H. Indeed, the distance across the dislocation core between Ga atoms in columns A and E is 2.85 Å, which is comparable to the 2.5–2.7 Å Ga-Ga distances in bulk Ga metal. Our results are at variance with earlier ones based on hydrogen-terminated clusters [9]. Such clusters possess band gaps exceeding the experimental ones. Empty dislocation bands, especially those with a broad dispersion as

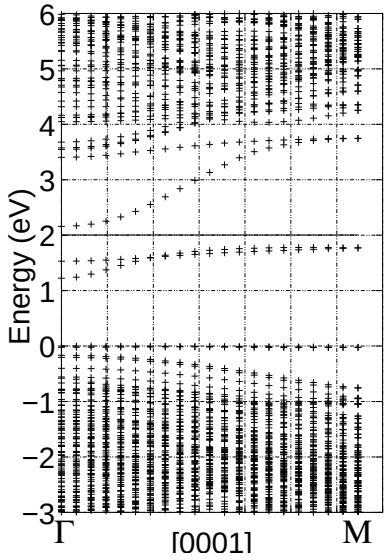

FIG. 3: Band structure in the [0001] c-direction of an edge dislocation charged with 2 electrons/c, calculated with the supercell shown in Fig. 2a, but with the atoms relaxed in the charged state. The solid horizontal line separates filled and empty states.

found here, can be then confused with conduction band states.

By comparing the band structures obtained here using the two approaches to describe an edge dislocation, some differences can be seen, although empty and filled bands are always in the same part of the gap. In approach (a), the strain induced by the dislocations is over-estimated with respect to an isolated dislocation in an otherwise perfect infinite crystal because of the computationally-restricted supercell size. Conversely, in approach (b), because the supercell surface is free to relax entirely, the dislocation strain is underestimated, and creates a bending of the $(10\bar{1}0)$ atomic planes parallel to the Burgers vector. This distortion is responsible, for example, for creating an artificially-raised filled level $\sim$0.4 eV above the valence band (see lower right panel of Fig. 2). These results conclusively show that neutral edge dislocations, expected to be present in p-type material, possess levels in the gap that lead to supplementary EELS absorption. The presence of dislocation-related gap states has recently been confirmed experimentally [33].

In Fig. 3, we show the band structure of a negatively-charged full-core edge dislocation, with 2 electrons per repeat distance (c) on the core of the dislocation. This is the charge state that has been observed by electron holography [7]. The addition of electrons to the dislocations is stabilised by a change in atomic structure that lowers the localized gap states of the neutral dislocation, pushing them deeper into the gap. The change in structure has been reported previously, and consists of a repulsive outward movement of the N atoms in columns A, E, F, and D and an attractive inward movement of the Ga atoms in these columns in the 8-fold ring at the dislocation core [10].

The computed energy-loss spectrum for the neutral edge dislocation is presented in Fig. 4. In view of the gap states created by the edge dislocation, additional absorption in the EEL spectrum is found below the bulk band edge. Absorption with the electron beam in the basal plane is seen to lead to absorption at lower energies than with the beam oriented along the c axis. Some supplementary absorption is also observed in the 5–7 eV range. Comparing the results obtained using the supercell and hybrid approaches gives

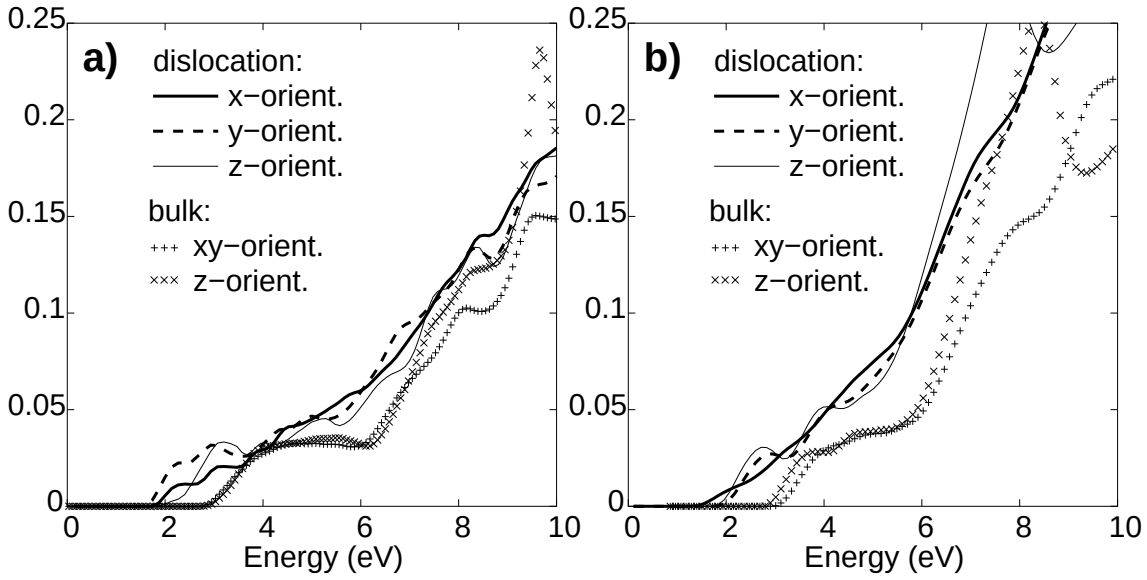

FIG. 4: Comparison between the computed EEL spectra of a region containing a neutral GaN edge dislocation (lines) and bulk GaN (symbols). The results are shown for the two units cells with dislocations shown in Fig. 2. In panel b, the dislocation EEL spectrum is compared with a bulk spectrum determined in a similar bulk hybrid supercell. In panel b, the spectra have been rescaled to account for the vacuum region in the supercell. Results are given for an electron beam oriented along x, y, and z, using the coordinate system defined in Fig. 2.

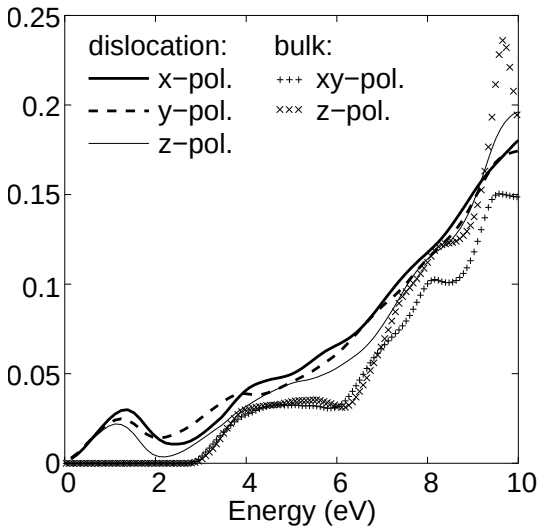

FIG. 5: Comparison between the computed EEL spectra of a region containing a negatively-charged GaN edge dislocation (lines) and bulk GaN (symbols), calculated using the supercell shown in Fig. 2a, but with the dislocation structure relaxed in the charged state. The dislocation carries a charge of 2 electrons/c. Results are given for an electron beam oriented along x, y, and z, using the coordinate system defined in Fig. 2.

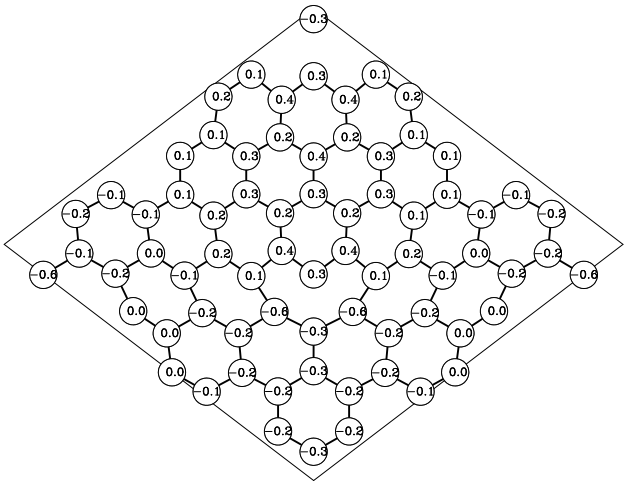

FIG. 6: Core-level energy differences $\Delta E_{\mathbf{R}}$, defined in the text, at nitrogen atoms near a neutral edge dislocation in GaN. Only the N atoms in the supercell are shown, projected in the (0001) plane. The potentials are given in eV with respect to the average value $\overline{E}$ of the potential at all N atoms in the supercell.

some idea of the accuracy of our modelled spectra. We note that the hybrid approach leads to a spectrum which rises more strongly above 6 eV, although the changes in absorption compared with bulk are similar to those found in Fig. 4a. These results make visible the importance of boundary conditions when calculating the electronic properties of dislocations. The computed EEL spectrum for a negatively-charged edge dislocation is shown in Fig. 5. The absorption in the band gap for all three orientations of the electron beam is shifted to lower energies compared to the neutral charge state, and consists of a broad peak centered around 1 eV.

In Fig. 6, we display the shifts of the N core levels near a neutral edge dislocation. We see that atoms in the compressive region near the dislocation, in columns A, B, and H, for example, have a shallower core level than those in the tensile region, such as columns D, E, and F. These potential shifts broaden the core EEL spectra taken on the dislocation. Fig. 7 shows the theoretical EEL spectrum for a dislocation compared with a bulk region. The dislocation spectrum is obtained by summing over core excitation from all the N atoms shown in Fig. 6. Near the dislocation, substantial absorption is found within the bulk band gap. We also note that the peaks in the bulk spectrum are smeared out. For charged dislocations, we expect an even stronger smearing of the peaks in view of the supplementary potential changes on the N cores induced by a line of charge. Therefore, core excitation EEL spectra should be interpreted with caution, as absorption seen below the conduction band edge does not necessarily imply the presence of an empty gap state at that energy in the band gap.

CONCLUSIONS

In this paper, we have computed from first principles the low-loss electron energy-loss spectra of bulk GaN and AlN, and found good agreement with recent experimental data. We have examined the effect of edge dislocations on the EEL spectra of GaN in a variety

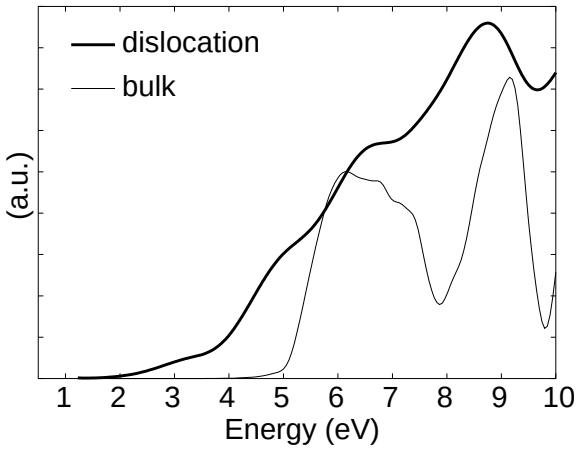

FIG. 7: Theoretical nitrogen K-edge core-level spectrum for an edge dislocation (thick line), in neutral or p-type material, compared to a similar bulk spectrum (thin line).

of charge states. Due to a change in core structure, a full-core negatively-charged edge dislocation is stabilized in n-type material. We find that undecorated full-core edge dislocations invariably lead to supplementary energy absorption within the band gap, which should be observable experimentally with an electron probe precisely positioned on the dislocation core. Nevertheless, one must bear in mind that there is a tradeoff in low-loss EEL measurements between deep levels on one hand, which create strong changes in the EEL spectra but are very localized and hard to pinpoint spatially, and shallow levels on the other hand, which lead to smaller changes in absorption, but are easier to place spatially. The model developed here of core-excitation EEL spectra acquired near edge dislocations has shown that the potential variations at the cores of nitrogen atoms near dislocations are strong, on the order of 1 eV. These variations smear out any sharp peaks in core EEL spectra and must be accounted for when interpreting core-excitation experiments.

The authors would like to thank A. Gutiérrez-Sosa and U. Bangert, for stimulating discussions and for providing the experimental EEL spectra.

---

* Electronic address: jones@excc.ex.ac.uk

[1] S. C. Jain, M. Willander, J. Narayan, and R. Van Overstaeten, J. Appl. Phys. **87**, 965 (2000).
[2] P. Vennéguès, B. Beaumont, M. Vaille, and P. Gibart, Appl. Phys. Lett. **70**, 2434 (1997).
[3] Z. Lilienthal-Weber, Y. Chen, S. Ruvimov, and J. Washburn, Phys. Rev. Lett. **79**, 2835 (1997).
[4] Y. Xin *et al.*, Appl. Phys. Lett. **72**, 2680 (1998).
[5] J. W. P. Hsu *et al.*, Appl. Phys. Lett. **78**, 3980 (2001).
[6] D. M. Schaadt, E. J. Miller, E. T. Yu, and J. M. Redwing, Appl. Phys. Lett. **78**, 88 (2001).
[7] D. Cherns and C. G. Jiao, Phys. Rev. Lett. **87**, 205504 (2001).
[8] H.-J. Im *et al.*, Phys. Rev. Lett. **87**, 106802 (2001).
[9] J. Elsner *et al.*, Phys. Rev. Lett. **79**, 3672 (1997).

[10] A. F. Wright and U. Grossner, Appl. Phys. Lett. **73**, 2751 (1998).
[11] K. Leung, A. F. Wright, and E. B. Stechel, Appl. Phys. Lett. **74**, 2495 (1999).
[12] S. M. Lee *et al.*, Phys. Rev. B **61**, 16033 (2000).
[13] J. E. Northrup, Appl. Phys. Lett. **78**, 2288 (2001).
[14] A. Nagayama *et al.*, to appear in phys. stat. sol. (unpublished).
[15] A. Gutiérrez-Sosa *et al.*, proceedings of the Royal Microscopic Society meeting, March 2001 (to be published).
[16] P. E. Batson, Phys. Rev. Lett. **83**, 4409 (1999).
[17] J. Bruley and P. E. Batson, Phys. Rev. B **40**, 9888 (1989).
[18] P. R. Briddon and R. Jones, Phys. Status Solidi B **217**, 131 (2000).
[19] G. B. Bachelet, D. R. Hamann, and M. Schlüter, Phys. Rev. B **26**, 4199 (1982).
[20] Y.-N. Xu and W. Y. Ching, Phys. Rev. B **48**, 4335 (1993).
[21] A. F. Wright and J. S. Nelson, Phys. Rev. B **50**, 2159 (1994).
[22] M. Leszczynski *et al.*, Appl. Phys. Lett. **69**, 73 (1996).
[23] J. Singh, *Physics of semiconductors and their heterostructures* (McGraw-Hill, New York, 1993).
[24] M. Ueno *et al.*, Phys. Rev. B **49**, 14 (1994).
[25] M. Ueno, A. Onodera, O. Shimomura, and K. Takemura, Phys. Rev. B **45**, 10123 (1992).
[26] J. R. K. Bigger *et al.*, Phys. Rev. Lett. **69**, 2224 (1992).
[27] M. Elstner *et al.*, Phys. Rev. B **58**, 7260 (1998).
[28] D. Nozières and D. Pines, Phys. Rev. **113**, 1254 (1959).
[29] G. F. Bassani and G. Pastori Parravicini, in *Electronic states and optical transitions in solids*, Vol. 8 of *International series of monographs in the science of the solid state*, edited by R. A. Ballinger (Pergamon Press, Oxford, 1975).
[30] A. J. Read and R. J. Needs, Phys. Rev. B **44**, 13071 (1991).
[31] W. R. L. Lambrecht *et al.*, Phys. Rev. B **51**, 13516 (1995).
[32] L. X. Benedict *et al.*, Solid State Commun. **112**, 129 (1999).
[33] A. Gutiérrez-Sosa and U. Bangert, private communication (unpublished).